CHAOTIC AND QUASIPERIODIC SOLUTIONS OF ROBOTIC EQUATION WITH ONE DEGREE OF FREEDOM

VLADIMIR PAAR

Department of Physics, Faculty of Science, University of Zagreb, 41000 Zagreb, Croatia

Received 10 January 1992

UDC 621.3.018

Original scientific paper

For the first time a possibility of chaotic regime for a robotic equation is investigated, using equation for a model of robot with one degree of freedom with viscous and dry friction and hard-spring rigidity. The transient motion was not excluded in this investigation. A chaotic regime is discovered in a particular scan, with enhanced rigidity, for the critical length parameter L_c which exceeds the upper limit of L in the standard parameter range by a factor of ≈ 50. In the chaotic regime a pronounced period three window is found.

1. Introduction

The concept of chaos in physics means that the system obeys deterministic laws of evolution, but the outcome is highly sensitive to small uncertainties in the specification of the initial state. In a chaotic system any small open ball of initial conditions, no matter how small, will in time spread over the phase space. Poincare was the first who indicated the possibility of such behaviour in dynamical systems[1]. Smoluchowski expressed the condition for applicability of the probabilistic conception to deterministic dynamical system by the famous phrase: »little cause — big effects«[2]. However, only in the recent time the large-scale applications of computer simulations enabled the progress in this field. The first results have been chaotic solutions found in computational calculations for some simple low-dimensional systems: a simplified model of atmospheric convection (Lorenz model)[3], a simplified model for the motion of stars in the center of galaxy[4] and

the model of electric circuit with nonlinear inductance under the impression of a sinusoidal voltage[5].

In the last two decades the topic of chaotic motion has found aboundant applications in a wide variety of physical phenomena, for example the problems of turbulence in fluids[6], buckling beams[7], nonlinear wave interactions in plasma[8], chemically reacting systems[9], charge density waves in solids[10], laser modulation[11], magnetodynamic flow[12], sound emitting[13] etc.

One-dimensional nonlinear systems present an important class of dynamical systems since there is an abundance of such systems in science and technology. In spite of much work being done in investigations of these systems it is still far from complete understanding of their dynamical behaviour. Most of the attention has been devoted to periodically driven damped nonlinear oscillators, and in particular to the Duffing oscillator[5,7,14-48]. Duffing system represents dynamics of various physical systems, as for example a buckled beam[7,15-17,24-26], nonlinear electrical circuits[5,14,20,33], charge density waves in solids[10], modulated laser[27,49] etc. Other one-dimensional systems being investigated comprise a periodically driven damped pendulum[50] which is isomorphic to a current driven Josephson junction[51-58] and to transport in charge-density-wave systems[58], Toda-oscillator[59,60], impact oscillator[61], van der Pol oscillator[62] and Morse and cavitation bubble models[63,64]. The practical importance of forced dynamical systems shows up in many applications, for example, in the case of periodically stimulated cardiac cells driven by a sinusoidal current[65] and the membranes of nerve cells driven by a sinusoidal current[66].

In general, varying control parameters of a nonlinear system a wide variety of periodic, subharmonic, quasiperiodic and chaotic motion can be obtained. It was found that there are several possible routes to chaos, including Feigenbaum period doubling[67], intermittency[68], quasiperiodic route[69] and crisis[70].

2. *Equation of motion for a simple robot with one degree of freedom*

An important point in engineering is that if one chooses parameters which produce chaotic output, then one loses predictability. Therefore it is important to search for the range of parameters for which chaos may occur.

In the present paper a possibility of chaotic regime is investigated for a simple model of a robot with one degree of freedom, described by the equation of motion[71-74]:

$$\ddot{x} - \beta_2 \dot{x}^2 - \gamma_2 \cdot \Theta_\varkappa(|\dot{x}|) \cdot \operatorname{sign}(\dot{x}) - \delta_{21} x - \delta_{23} x^3 =$$

$$= L \frac{\omega_0^2}{2\pi} \cos(\omega_0 t) - \xi_{21} e^{\lambda_{21} t} - \xi_{22} e^{\lambda_{22} t} \tag{1}$$

with

$$\Theta_\varkappa(|\dot{x}|) = \begin{cases} 1 & , \text{ if } \varkappa\dot{x}| \geq 1 \\ |\varkappa\dot{x}| & , \text{ if } |\varkappa\dot{x}| < 1. \end{cases} \tag{2}$$

The second and third term on the l. h. s. of Eq. (1) are dissipative terms, corresponding to viscous and dry friction, respectively. The damping function (2) in dry friction was introduced here in order to enable numerical integration of Eq. (1). In the calculation the value $\varkappa = 10$ is used; generally, the value of $\varkappa$ should increase with increasing value of the dry friction parameter γ_2. The parameters δ_{21} and δ_{23} are the coefficients of rigidity and $\delta_{21} < 0$, $\delta_{23} < 0$ correspond to the rigidity with the effect of a hard spring. The first term on the r. h. s. of Eq. (1) is the periodic driving force with driving frequency ω_0 and driving amplitude $L\frac{\omega_0^2}{2\pi}$ where L denotes the length. This term corresponds to the control minimizing the Hamiltonian[75]. The last two terms present the initial drive with strengths given by

$$\xi_{21} = \frac{a_2}{c_2} \cdot \lambda_{21}^2$$

$$\xi_{22} = \frac{b_2}{c_2} \cdot \lambda_{22}^2$$

$$a_2 = (\lambda_{22} - 1) \cdot z_2 \qquad (3)$$

$$b_2 = (1 - \lambda_{21}) \cdot z_4$$

$$c_2 = \lambda_{22} - \lambda_{11}.$$

The parameters λ_{21} and λ_{22} denote the roots of the system in the regime of closed regulation loop. A more descriptive formulation of the model (1) and investigation of sensitivity of solutions to the perturbation terms will be presented elsewhere[74]. In the present paper we report preliminary results of the investigations of possible chaotic solutions associated with the robotic equation (1). It is obvious that the rigidity terms on the r. h. s. of Eq. (1) can be relevant only in the transient regime, but not in the stationary one. Thus, there are three nonlinearities giving rise to the chaotic behaviour: the cubic anharmonicity (the δ_{23}-term), the viscous friction (the β_2-term) and dry friction (the γ_2-term). In the present preliminary investigation we have fixed the strengths of these nonlinearities within the realistic range, while the investigation of their relative importance will be presented in a forthcoming publication. A further comment is needed regarding relation of the model (1) to the Duffing oscillator. The dry-friction term for small values of $|\dot{x}|$ resembles the friction in Duffing oscillator, while for the values larger than $\frac{1}{\varkappa}$ it stays constant, which is the basic difference with respect to the behaviour of the corresponding term in Duffing model. Furthermore, the viscous term in the robotic model (1) has no counterpart in the Duffing model.

3. *Calculation of Poincare maps and power spectra for robotic equation in a scan with enhanced rigidity and variable length*

The robotic equation (1) is solved numerically and the solutions are investigated using three descriptors: phase portrait, Poincare map and power spectrum.

In comparison to the one-dimensional systems investigated previously from the point of view of chaos, the system (1) is characterized by some completely novel features: the viscous and dry friction and the initial drive The influence of these interactions on the chaotic behaviour was not considered so far.

The equation (1) is cast in the form of an autonomous system

$$\begin{aligned} \dot{x} &= y \\ \dot{y} &= \beta_2 y^2 + \gamma_2 \Theta_*(|y|) \operatorname{sign}(y) + \delta_{21} x + \delta_{23} x^3 + \\ &\quad + L \frac{\omega_0^2}{2\pi} \cos z - \xi_{21} e^{\frac{\lambda_{21}}{\omega_0} z} - \xi_{22} e^{\frac{\lambda_{22}}{\omega_0} z} \\ \dot{z} &= \omega_0 \end{aligned} \tag{4}$$

with $z(0) = 0$. This system was integrated using the fourth-order Runge-Kutta method[77].

The shape of potential in Eq. (1) is responsible for globally bounded solutions, for $V(x) \to \infty$ as $x \to \infty$. A specific feature of this potential is the existence of a single well. In this connection one should note that the single-well Duffing system revealed the existence of chaotic solutions in spite of the absence of homoclinic orbit for the unperturbed problem.

We have first investigated the robotic equation (1) for parameters within the standard range[74], corresponding to a realistic robot model. In accordance with the expectations, the system governed by Eq. (1) is in the periodic regime: it shows a limit cycle behaviour with the period of driving force.

In a search for a possible chaotic regime in the state space of the robotic equation (1), the following scanning outside the standard parameter range is employed: The length parameter L is treated as a control parameter. The standard range is $0 \leq L \leq 1$. The other model parameters are fixed at the values: $\omega_0 = 2\pi$, $\lambda_{21} = -10.5$, $\lambda_{22} = -11.5$, $\xi_2 = 0.01$, $\xi_4 = 0.01$, $\beta_2 = -5.18 \cdot 10^{-6}$, $\gamma_2 = -0.00298$, $\delta_{21} = -0.7611$, $\delta_{23} = -0.0127$ which will be referred to as parametrization (I). It should be noted that in this scan $\gamma_2 = 2.5 \cdot \delta_2$ (min), $\delta_{21} = 10\delta_{21}$ (min), $\delta_{23} = 10\delta_{23}$ (min), where the labels min stand for the lower limits of the standard parameter range[74]. The values of other parameters in (I) lie within the standard parameter range. Initial conditions in the calculation are naturally $x_0 = 0$, $\dot{x}_0 = 0$.

Phase portraits, Poincare maps and power spectra have been calculated in the scan (I) with the control parameter L varied from $L = 0.1$ to $L = 100$. The characteristic results of calculations are presented in Figs. 1 and 2 for Poincare maps and power spectra, respectively. It is evident that the $L = 49$ and $L = 99$ cases are chaotic, while the situation for other values of L presented in Figs. 1, 2 corresponds to a quasiperiodic motion. Furthermore, it turns out that in the proposed scan the system is characterized by transients of long duration which increases with increasing L. Thus, it should be noted that the most of the points in some figures belong to the transient regime, so that the attractors are not clearly extracted from their basins. Consequently, the accompanying power spectra exhibit a superposed transient nd stationary pattern. For example, in Figs. 1.a—d all

Fig. 1 (a)

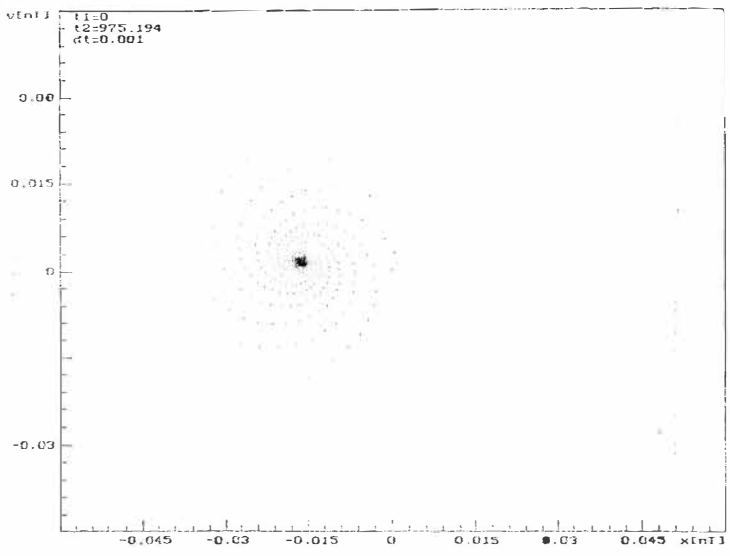
t1=0
t2=975.194
dt=0.001
0.06
0.015
0
-0.03
-0.045
-0.03
-0.015
0
0.015
0.03
0.045
x[nT]

Fig. 1 (b)

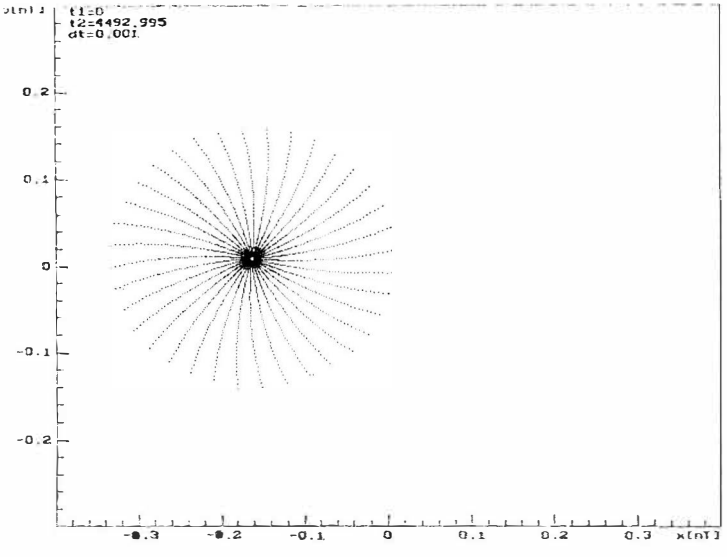
t1=0
t2=4492.995
dt=0.001
0.2
0.1
0
-0.1
-0.2
-0.3
-0.2
-0.1
0
0.1
0.2
0.3
x[nT]

Fig. 1 (c)

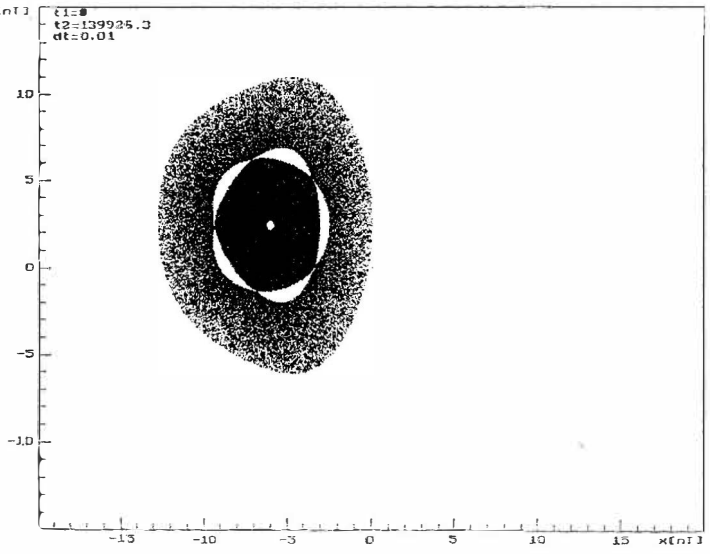
t1=0
t2=139925.3
dt=0.01
y[nT]
x[nT]
10
5
0
-5
-10
-15
-10
-5
0
5
10
15

Fig. 1 (d)

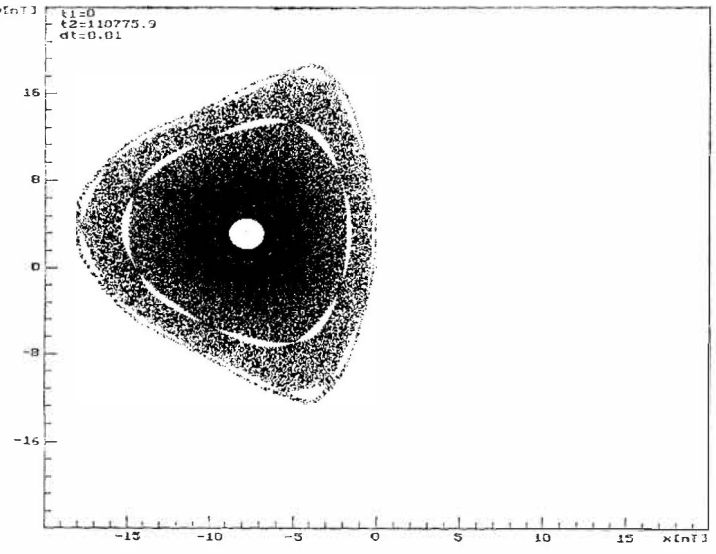
t1=0
t2=110775.9
dt=0.01
y[nT]
x[nT]
16
8
0
-8
-16
-15
-10
-5
0
5
10
15

Fig. 1 (e)

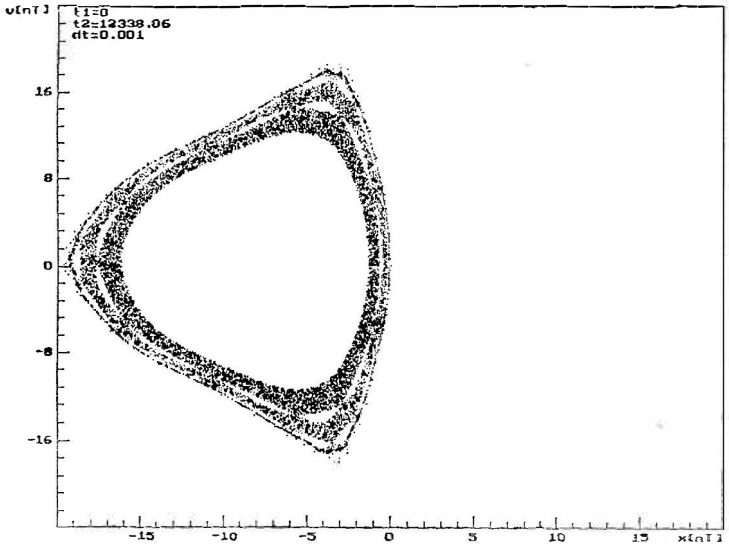
v[nT]
t1=0
t2=12338.06
dt=0.001
16
8
0
-8
-16
-15
-10
-5
0
5
10
15
x[nT]

Fig. 1 (f)

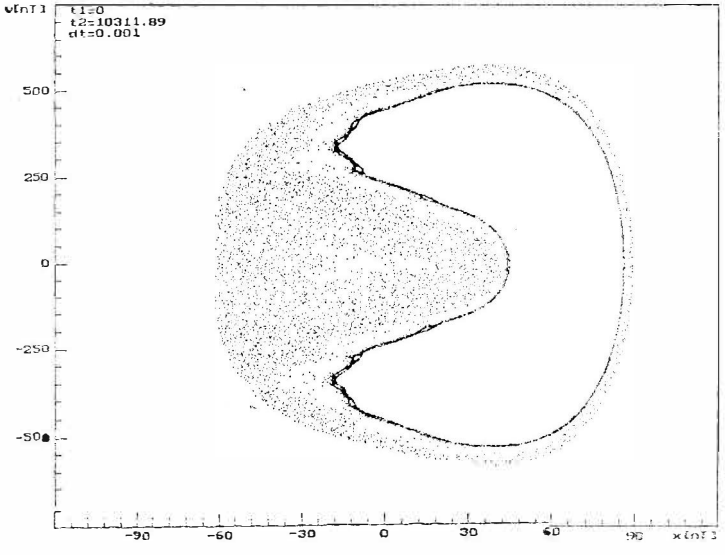
v[nT]
t1=0
t2=10311.89
dt=0.001
500
250
0
-250
-500
-90
-60
-30
0
30
60
90
x[nT]

Fig. 1 (g)

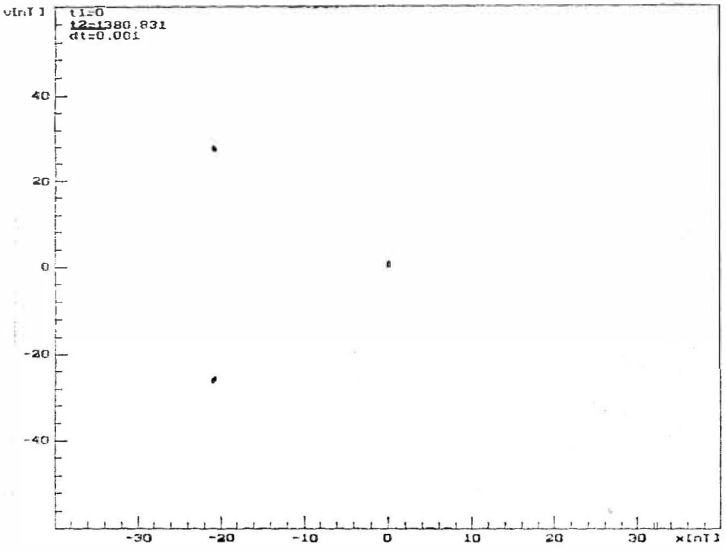

Fig. 1 (h)

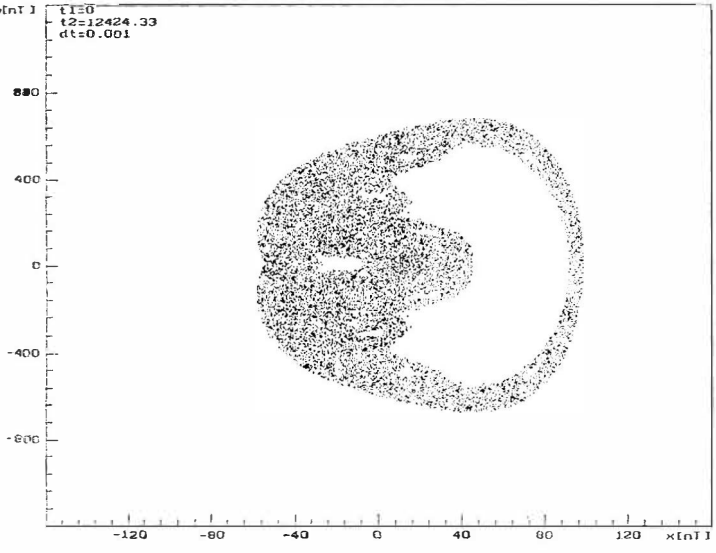

Fig. 1. Poincare maps for robotic equation (1) with parametrization (I) and the characteristic values of the control parameter L: (a) $L = 0.1$, (b) $L = 1$, (c) $L = 37$, (d) $L = 47$, (e) $L = 48$, (f) $L = 49$, (g) $L = 74$, (h) $L = 99$.

In the upper left corner t_1 and t_2 denote the initial and final time of the evolution of orbit presented in figure and dt denotes the time interval employed in numerical integration. Each Poincare map is obtained by considering the surface of sections in the phase plane $(x, \dot{x})$ at times when $\omega_0 t = 2\pi n$, where $n = 0, 1, 2, 3, \ldots$.

points belong to the transient regime which is of a very long duration. Thus, the parallel is drawn between the transient regime of the robotic model (1) and the periodic attractor of the Curry-Yorke mapping. In this way, this comparison relates different physical regimes, and strictly speaking it is not necessary to introduce the complete definition of the model (5). Thus, in the comparison considered, here, the formula of Curry-Yorke model should be considered only as a convenient parametrization for the present results of the transient regime.

4. *Quasiperiodic and chaotic regime for L-scan with increased rigidity*

Poincare maps in Figs. 1 (a)—(d) are characterized by one attracting point for the transient pattern. Fig. 1 (a) ($L = 0.1$) exhibits pseudosymmetry of order seven. Namely, starting from the initial point (0, 0) in the clockwise direction, the following seven points (labelled (1—7)) lie approximately on a circle. The following point (8) is placed near the point of departure in the first sequence (1), but is slightly shifted in the clockwise direction and closer to the attracting point. The points 8—14 of the second sequence lie approximately on a circle centered at the attracting point, of slightly smaller radius than for the circle of the first sequence and each point is slightly shifted in the clockwise direction. An analogous structure appears for the third sequence of points (15—21) with still smaller radius etc. As a result the points appear to lie on seven curved lines spiralling towards the attracting point (Fig. 1 (a)). Such a pattern resembles (in a sense discussed in the previous section) the result of the mapping given by the composition of two homomorphisms of the type introduced in the Curry-Yorke model[80]:

$$\psi = \psi_1 \circ \psi_2$$

$$\psi_1 = \begin{cases} \varrho_{k+1} = \varepsilon \ln (1 + \varrho_k) \\ \Theta_{k+1} = \Theta_k + \bullet_0 \end{cases} \tag{5}$$

$$\psi_2 = \begin{cases} X_{k+1} = X_k \\ Y_{k+1} = Y_k + X_k^2. \end{cases}$$

Here, $\circ$ denotes the composition of mappings: ψ_1 defines, in polar coordinates $(\varrho, \bullet)$, the $(k+1)$-st iterate as a function of the k-th, $\varepsilon \geq 0$, $\Theta_0 > 0$ are the control parameters and initial values are $\varrho \ll 1$ and Θ_1; Ψ_2 relates the Cartesian coordinates (X, Y) of two consecutive iterates. For $\Theta_0 \approx \frac{2\pi}{7}$ the mapping (5) gives the pattern which is similar to the Poincare map 1 (a). Furthermore, the pseudosymmetry of order seven is consistent with the power spectrum which exhibits two fundamental frequencies, the driving frequency ω_0 and the frequency of the system, labelled ω_1. For $L = 0.1$ the calculation of Fourier spectrum gives $\omega_0/\omega_1 \approx 7.39$.

It should be noted that ω_1 ($L = 0.1$) is close to the frequency of undriven system ω_1 ($L = 0$) $\approx 7.46\,\omega_0$. In the range of control parameter L between $L =$

$= 0.1$ and $L = 48$ the qausiperiodic regime with two pronounced freqeuncies persists and the frequency of the system, ω_1, is slowly increasing with L: the ratio ω_0/ω_1 gradually decreases from $\omega_0/\omega_1 \approx 7.39$ to $\omega_0/\omega_1 \approx 3.5$. As a guideline, for $L \lesssim 48$ one can use an estimate

$$\frac{\omega_0}{\omega_1} = -0.7\, L + 7.3. \tag{6}$$

The Poincare map for $L = 1$ (Fig. 1 (b)) has a more complex structure than for the $L = 0.1$ case: Along the outer circle there are five intertwinned sequences, seven points each. Moving in the clockwise direction, the seven points of the first sequence (labelled 1—7) are regularly placed on the circle, in a similar way as in the previous case. The next sequence of seven points, however, lies on the same circle, each point being shifted in the counter-clockwise direction, by a polar angle of $\approx \frac{2\pi}{36}$, from the position of the corresponding point of the first sequence. In analogy, the points of the next three sequences move approximately along the same circle. Thus, one obtains a pattern consisting of 36 points, almost uniformly distri buted on the circle in the order of appearance 1, 30, 23, 16, 9, 2, 31, 24, 17, 10, 7, 36, 29, 22, 15, 8. The spacing between each pair of neighbouring points is approximately equal along the outer circle. The following six sequences of points, 37, 66, 59, 52, 45, 38,... appear near the points 1, 30, 23, 16, 9, 2,..., respectively, but closer to the attracting point; they lie on the first inner circle.

Density of points in the spiralling inward structure rapidly increases with the control parameter L, and tends to uniformly fill up a section of the phase plane. Hence, a difference between chaotic and quasiperiodic motion may not be evident from the Poincare map alone. In the present quasiperiodic case the motion of point is not random, although they fill a section of the phase plane; the points progress along dense spirals. This transient motion is of long duration so that even after rather long time there remains an empty central circular region around the attracting point, as seen in Figs. 1 (c)—(e).

Power spectra in the control parameter range up to $L = 48$ show a quasiperiodic behaviour with two fundamental frequency, as already noted. For $L=37$ and $L = 47$ in the power spectrum (Figs. 2 (c) and (d), respectively) the ratio of two fundamental frequencies is $\omega_0/\omega_1 \approx 4.7$ and $\omega_0/\omega_1 \approx 3.6$, respectively. In addition, in both cases one observes a weak peak ($\approx 10^{-4}$ of the strength of two fundamental frequencies) at the combination frequency $\approx \omega_0 - 2\omega_1$. For $L = 47$ one observes three even weaker peaks which are close to the combination frequencies $4\omega_1 - \omega_0$, $2\omega_0 - 5\omega_1$ and $3\omega_1$, respectively.

Another feature of Poincare maps in the quasiperiodic regime is the appearance of islands. For $L = 37$ there appears one chain of five islands, in accordance with $\omega_0/\omega_1 \approx 5$. For $L = 47$ we find two chains of islands, the outer chain composed of 11 islands and the inner of 8 islands. For $L = 48$ we observe three chains of islands. In the last case however, a signature of a close-lying chaotic motion (at $L = 49$) can be detected: around the three corners of the map pattern there appear some random points, in particular during the initial transient motion, while the chains of islands become more compressed and with less regular boundaries.

For $L = 49$ we find the first appearance of chaos when the control parameter L increases along the parameter scan used in this paper. This chaotic Poincare map (Fig. 1 (f)) exhibits a finer structure: it consists of a chaotic transient characterized by a random distribution of points on the accessible surface, similar to a cloud of unorganized points obtained in the case of Hamiltonian or low-dissipation systems[81]. On the other hand the chaotic asymptote for $L = 49$ resembles the shape of a strange attractor characteristic for dissipative systems in the chaotic regime. The power spectrum in Fig. 2 (d) shows a broad-band structure typical of chaotic motion.

On the basis of these calculations, it seems that the possible scenario for the route to chaos could be: fixed point → limit cycle → quasi-periodic two-dimensional thorus → strange attractors, with periodic windows after. In the present consideration we include the transient regime and therefore the precise value of the critical parameter L is influenced by the transient behaviour. In the forthcoming investigation we will investigate in more details the neighborhoods of critical points in the stationary regime.

Further increasing the control parameter L, the system (1) stays in the chaotic regime until the appearance of a pronounced periodic window at $L = 74$. (However, possible existence of some narrow periodic windows which do not show up in the present scan, with $\Delta L = 1$, cannot be excluded.) The corresponding Poincare map (Fig. 1 (g)) and power spectrum (Fig. 2 (e)) show a pronounced period three frequency locking: Poincare map is close to a three-point system and the ratio of fundamental frequencies in the power spectrum is $\omega_0/\omega_1 \approx 3$. In this connection it should be pointed out that in the mathematical literature much attention has been attached to the period three modes generated beyond the chaotic region[82].

For the values of control parameter L above this periodic window the chaotic motion appears again. As an example, in Figs. 1 (h) and 2 (f) the Poincare map and power spectrum for $L = 99$ are presented.

Fig. 2 (a)

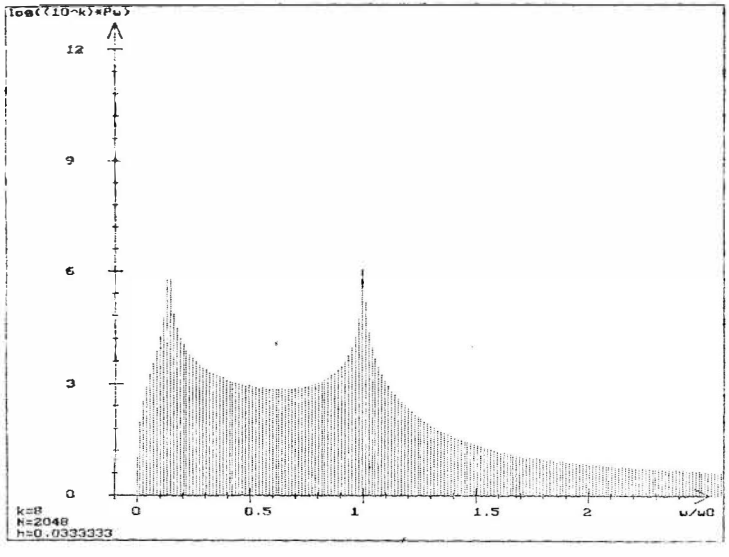

Fig. 2 (b)

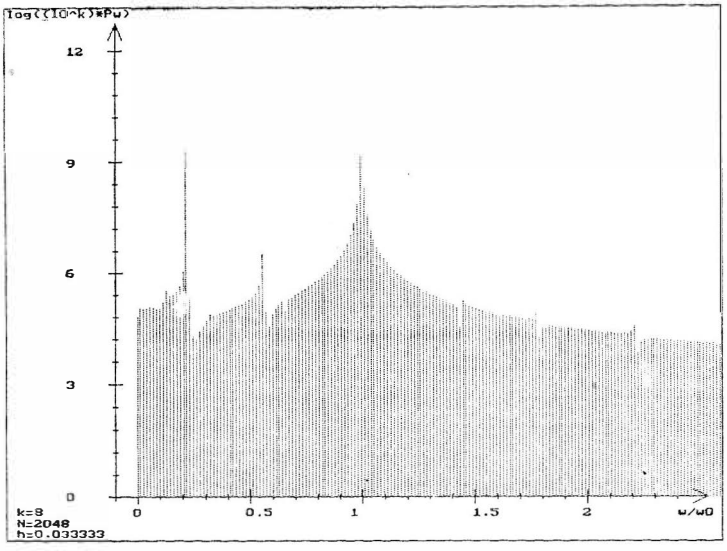
log((10^k)*Pw)
12
9
6
3
0
k=8
N=2048
h=0.033333
0
0.5
1
1.5
2
w/w0

Fig. 2 (c)

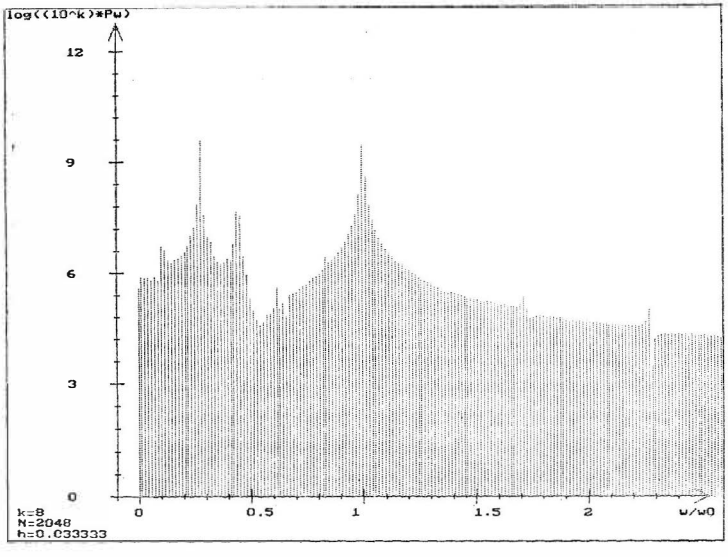
log((10^k)*Pw)
12
9
6
3
0
k=8
N=2048
h=0.033333
0
0.5
1
1.5
2
w/w0

Fig. 2 (d)

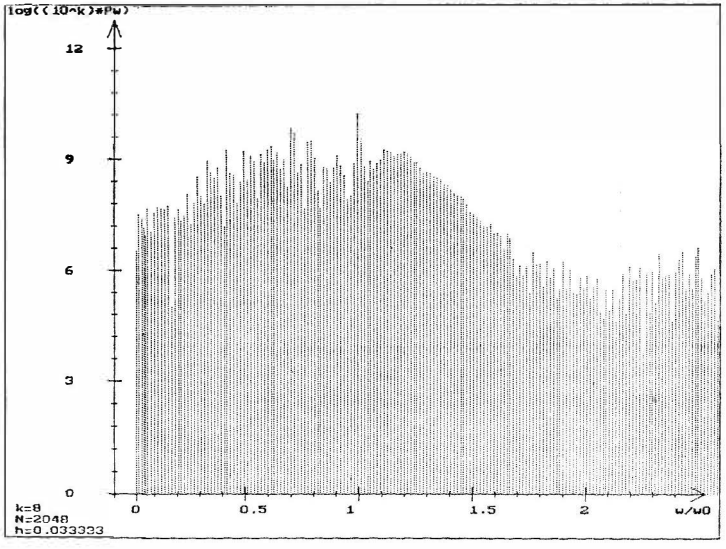
log((10^k)*Pw)
12
9
6
3
0
0
0.5
1
1.5
2
w/w0
k=8
N=2048
h=0.033333

Fig. 2 (e)

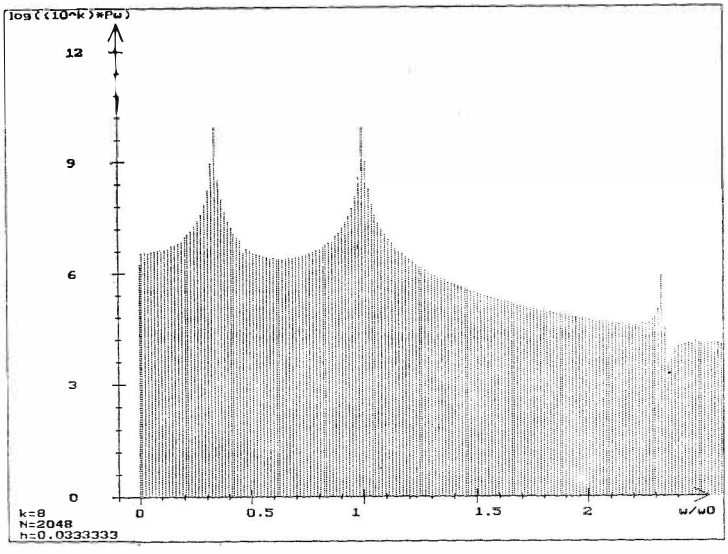
log((10^k)*Pw)
12
9
6
3
0
0
0.5
1
1.5
2
w/w0
k=8
N=2048
h=0.033333

Fig. 2 (f)

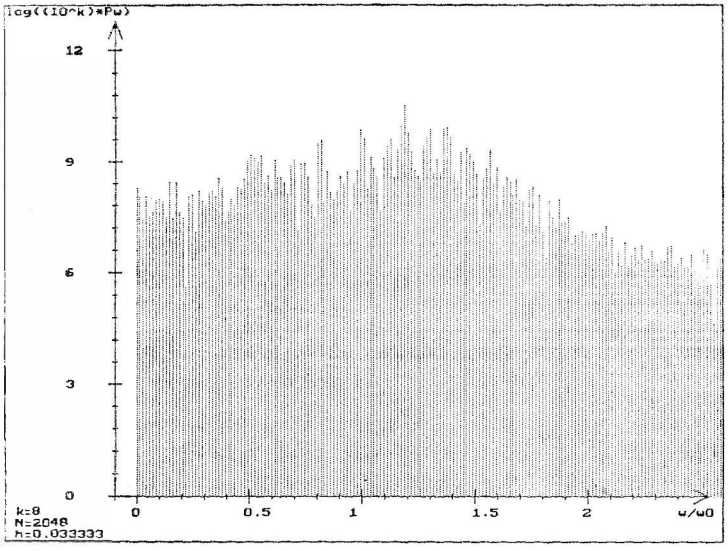

Fig. 2. Power spectra for solutions of robotic equation (1) with parametrization (I) and the characteristic values of the control parameter L: (a) $L = 1$, (b) $L = 37$, (c) $L = 47$, (d) $L = 49$, (e) $L = 74$, (f) $L = 99$. In each case, the Fourier analysis encompasses a time series consisting of $N = 2084$ elements, starting from $t_1 = 0$.

Fast Fourier transform (FFT) calculation was performed using N consecutive sampled values $x(t_k)$; $t_k = k \cdot \Delta$, $k = 0, 1, 2, \ldots, N-1$ where $N = 2^n$, $n =$ integer. The sampling time interval was $\Delta = T_0/30 = 2\pi/(30\omega_0)$. The periodogram estimate of the power spectrum for discrete Fourier transform C_k is defined at $\frac{N}{2} + 1$ frequencies as[77]:

$$P(0) = |C_0|^2/N^2$$

$$P(\omega_k) = (|C_k|^2 + |C_{N-k}|^2)/N^2, \qquad k = 1, 2, \ldots, \frac{N}{2} - 1$$

$$P(\omega_{N/2}) = |C_{N/2}|^2/N^2$$

where $\omega_k = \dfrac{k}{N\Delta}$.

It should be noted that the power spectra of chaotic motion for $L = 49$ and $L = 99$ do not show peaks of fundamental frequencies superimposed on the broad band. Furthermore, these power spectra do not obey the $1/\omega$ law for low frequency; the calculated distributions are closer to the white noise asymptote.

5. *Conclusions*

In the present paper we have investigated the one-dimensional robotic model (1), including the transient regime. Thus, the calculated Poincare sections and power spectra reflect the transients and the onset of the stationary regime. (In some cases of the fixed-point type, with very long transients, the moderate-size computation does not even reach the stationary regime.)

For the parameter scan used in this paper we have found a quasiperiodic route to chaos. A broad range of quasiperiodic motion is characterized by two incommensurate fundamental frequencies, ω_1 and ω_0, and below the critical value of control parameter L we observe in the power spectrum a weak peak of the third frequency at $\approx \omega_0 - 2\omega_1$. It remains to be seen whether this frequency is exactly the combination frequency built from the two fundamental frequencies or whether it is the third independent frequency giving rise to instability of the corresponding thorus and its replacement by a strange attractor due to Newhouse-Ruelle-Takens scenario[69]. As is well known, the third frequency may or may not be detectable in the spectrum before chaos is identified[83].

Another interesting question which requires further investigation is related to the asymptotic symmetry associated with invariance under transformation

$$x \to -x, \quad \dot{x} \to -\dot{x}, \quad t \to t + \frac{T}{2} \tag{7}$$

where T denotes the period of the driving force. The system (1) is invariant under the transformation (7) in the limit $t \to \infty$, $\beta_2 \to 0$. It should be noted that the Duffing and pendulum systems are exactly invariant under transformation (7)[19,28,58,84]. As a consequence of symmetry (7), even multiples of fundamental frequency should be absent in the power spectrum. Indeed, in the calculated power spectra no peak is observed at the frequency $2\omega_0$. Closer information on the effects of symmetry spectra in Fig. 2 is masked due to noise caused by truncation of the time series used in the present calculation of Fourier transforms.

We have found an illustration for symmetry (7) ($L = 99$ with all parameters taken as in the parametrization (I) except for driving frequency $\omega_0 = 3.283$) with a frequency locking of period five, showing peaks in the power spectrum at $\omega_0/5$, $3\omega_0/5$, ω, $7\omega_0/5$, $9\omega_0/5$ and $11\omega_0/5$. (The two highest peaks, corresponding to the fundamental frequencies are $\omega_0/5$ and ω_0). All even multiples of $\omega_0/5$, on the other hand, are missing in the power spectrum.

In the present paper the onset of chaos was investigated for a particular scan and the corresponding critical value of the control parameter $L_c = 49$ was found. It remains to be investigated what is a functional dependence of the critical value of control parameter on other quantities in the robotic equation, primarily on the frequency ω_0 and dissipation parameters β_0 and γ_0. One should search for a possible analogy with the Holmes criterion for Duffing system[7], which was based on the existence of homoclinic orbit in the unperturbed system. (As already noted, a straightforward generalization of this criterion is not possible, because of the absence of homoclinic orbit in the present case.)

A more complete investigation of the state diagram in the parameter space driving parameters (L, ω_0), with exclusion of transient motion, is in progress[74].

Acknowledgement

The author thanks to N. Paar for computational assistance.

References

1) H. Poincare *Les Méthodes Nouvelles de la Méchanique Celeste* (Gauthier-Villars, Paris, **1892**);
2) M. V. Smoluchowski, Naturwissenschaften **6** (1921) 253;
3) E. N. Lorenz, J. Atmos. Sci. **20** (1963) 130;
4) M. Henon and C. Heiles, Astron. J. (1964) 73;
5) Y. Ueda. N. Akamatsu and C. Hayashi, Electronics and Communications in Japan **56A** (1973) 27;
6) D. Ruelle and F. Takens, Commun. Math. Phys. **20** (1971) 167;
7) P. J. Holmes, Phil. Trans. Roy. Soc. **A292** (1979) 419;
8) J. M. Wersinger, J. M. Finn and E. Ott, Phys. Fluids **23** (1980) 1142;
9) J. L. Hudson and J. C. Mankin, J. Chem. Phys. **74** (1981) 6171;
10) B. A. Huberman and J. P. Cruchfield, Phys. Rev. Lett. **43** (1979) 1743;
11) H. Haken, Phys. Lett. **A53** (1975) 77;
12) Y. Treve and O. P. Manley, In *Intrinsic Stochasticity in Plasmas*, ed. G. Laval and D. Gresillon (Les Editions de Physique Courtaboeuf, Orsay, 1980), p. 393;
13) W. Lauterborn and U. Parlitz, J. Acoust. Soc. Am. **84** (1988) 1975;
14) Y. Ueda, J. Stat. Phys. **20** (1979) 181;
15) F. C. Moon and P. J. Holmes, J. Sound. Vib. **65** (1979) 275;
16) F. C. Moon, Trans. ASME, **47** (1980) 638;
17) C. Holmes and P. Holmes, J. Sound. Vib. **78** (1981) 161;
18) W. H. Steeb and A. Kunick, Phys. Rev. **A25** (1982) 2889;
19) S. Novak and R. G. Frehlich, Phys. Rev. **A26** (1982) 3660;
20) F. T. Arecchi and F. Lisi, Phys. Rev. Lett. **49** (1982) 94;
21) S. Sato, M. Sano and Y. Sawada, Phys. Rev. **A28** (1983) 1654;
22) J. N. Elgin and D. Forster, Phys. Lett. **94A** (1983) 195;
23) W. H. Steeb, W. Erig and A. Kunick, Phys. Lett. **93A** (1983) 267;
24) P. Holmes and D. Whitley, Physica **7D** (1983) 111;
25) P. J. Holmes and F. C. Moon, J. Appl. Mech. **50** (1983) 1021;
26) F. Moon, Phys. Rev. Lett. **53** (1984) 962;
27) F. T. Arecchi and A. Califano, Phys. Lett. **101A** (1984) 443;
28) R. Räty, J. von Boehm and H. M. Isomäki, Phys. Lett. **103A** (1984) 289;
29) F. C. Moon and G. X. Li, Phys. Rev. Lett. **55** (1985) 1439;
30) U. Parlitz and W. Lauterborn, Phys. Lett. **107A** (1985) 351;
31) F. T. Arecchi, R. Badii and A. Politi, Phys. Rev. **A32** (1985) 402;
32) F. T. Arecchi, Phys. Scr. **T9** (1985) 85;
33) Y. Ueda, Int. J. Non-Linear Mech. **20** (1985) 481;
34) K. Wiesenfeld and B. McNamara, Phys. Rev. Lett. **55** (1985) 13;
35) U. Parlitz and W. Lauterborn, Z. Naturforsch. **41A** (1986) 605;
36) H. Ishii, H. Fujisaka and M. Inoue, Phys. Lett. **116A** (1986) 257;
37) R. Räty, J. von Boehm and H. M. Isomäki, Phys. Rev. **A34** (1986) 4310;
38) Y. H. Kao, J. C. Huang and Y. S. Gou, Phys. Rev. **A35** (1987) 5228;
39) Y. H. Kao, J. C. Huang and Y. S. Gou, Phys. Lett. **131A** (1988) 91;
40) A. Yamaguchi, H. Fujisaka and M. Inoue, Phys. Lett. **135A** (1989) 320;
41) J. C. Huang, Y. H. Kao, C. S. Wang and Y. S. Gou, Phys. Lett. **136B** (1989) 131;
42) G. A. Ruseva and V. I. Medvedev, Bug. J. Phys. **16** (1989) 449;
43) T. Kapitaniak, Phys. Lett. **144B** (1990) 322;
44) C. Scheffczyk, U. Parlitz, T. Kurz, W. Knop and W. Lauterborn, Phys. Rev. **A43** (1991) 6495;
45) V. Englisch and W. Lauterborn, Phys. Rev. **A44** (1991) 916;
46) J. Guckenheimer and P. Holmes, *Nonlinear Oscillations, Dynamical System, and Bifurcations of Vector Fields* (Springer, New York, 1990);
47) W. Szemplinska-Stupnicka, G. Iooss and F. C. Moon, *Chaotic Motions in Nonlinear Dynamical Systems* (Springer, Wien, 1988);
48) C. Hayashi, *Nonlinear Oscillations in Physical Systems* (McGraw Hill, New York, 1964);
49) F. T. Arecchi, R. Meucci, G. F. Puccioni and J. Tredicce, Phys. Rev. Lett. **49** (1982) 1217;
50) D. D'Humieres, M. R. Beasley, B. A. Huberman and A. Libchaber, Phys. Rev. **A26** (1982) 3483;
51) R. L. Kautz, J. Appl. Phys. **52** (1981) 6241;
52) N. F. Pedersen and A. Davidson, Appl. Phys. Lett. **39** (1981) 830;
53) M. T. Levinsen, J. Appl. Phys. **53** (1982) 4294;
54) W. J. Yeh and Y. H. Kao, Appl. Phys. Lett. **42** (1983) 299;

55) H. Seifert, Phys. Lett. **98A** (1983, 213;
56) E. G. Gwinn and R. M. Westervelt, Phys. Rev. Lett. **54** (1985) 1613;
57) Y. H. Kao, J. C. Huang and Y. S. Gou, J. Low Temp. Phys. **63** (1986) 287;
58) A. H. Mac Donald and M. Plischke, Phys. Rev. **B27** (1983) 201;
59) T. Klinker, W. Meyer-Ilse and W. Lauterborn, Phys. Lett. **101A** (1984) 371;
60) M. Toda, Phys. Rep. **18** (1975) 1;
61) J. M. T. Thompson and R. Ghaffari, Phys. Rev. **A27** (1983) 1741;
62) U. Parlitz and W. Lauterborn, Phys. Rev. **A36** (1987) 1428;
63) U. Parlitz, V. Englisch, C. Scheffczyk and W. Lauterborn, J. Acoust. Soc. Am. **88** (1990) 1061;
64) W. Knop and W. Lauterborn, J. Chem. Phys. **93** (1990) 3950;
65) M. R. Guevara, L. Glass and A. Schrier, Science **214** (1981) 1350;
66) A. V. Holden, W. Winlow and P. G. Haydon, Biol. Cybernetics **43** (1982) 169;
67) M. J. Peigenbaum, J. Stat. Phys. **19** (1978) 25;
68) Y. Pomeau and P. Manneville, Commun. Math. Phys. **74** (1980) 189;
69) S. Newhouse, D. Ruelle and F. Takens, Commun. Math. Phys. **64** (1978) 35;
70) C. Grebogi, E. Ott and J. A. Yorke, Phys. Rev. Lett. **48** (1982) 1507;
71) E. Freund and H. Hoyer, Int. J. Robotic Res. **7** (1988) 42;
72) B. M. Novaković, Proc. Int. AMSE Conf. Signals and Systems (Brighton, AMSE Press, 1989) p. 175;
73) B. M. Novaković, AMSE Conf. Modell. and Simul. Proc. Vol. **3A** (Karlsruhe, 1987) p. 107;
74) V. Paar, N. Paar and B. M. Novaković, to be published;
75) F. Csaki, State Space Methods for Control Systems, (Akademia. Kiado, Budapest, 1977);
76) N. Paar, Computer code RKROBOT 3/C (1991);
77) W. X. Press, B. P. Flannery, S. A. Teukolsky and W. T. Vetterling, Numerical Recipes in C (Cambridge University Press, Cambridge, 1988);
78) C. Hayashi, Int. J. Non-Linear Mech. **15** (1980) 341;
79) Y. Ueda, Ann. N. Y. Acad. Sci **357** (1980) 422;
80) J. Curry and J. A. Yorke, Springer Notes in Mathematics **668** (1977) 48;
81) M. Henon, in *Chaotic Behavior of Deterministic Systems*, eds. G. Iooss R. H. G. Helleman and R. Stora (North-Holland, Amsterdam, 1983), p. 53;
82) T. Y. Li and J. A. Yorke, Am. Math. Monthly **82** (1975) 85;
83) P. Berge, Y. Pomeau and C. Vidal, *Order Within Chaos* (Wiley, New York, 1984);
84) J. W. Swift and K. Diesenfeld, Phys. Rev. Lett. **52** (1984) 705.

KAOTIČKA I KVAZIPERIODIČNA RJEŠENJA ROBOTIČKE JEDNADŽBE S JEDNIM STUPNJEM SLOBODE

VLADIMIR PAAR

Fizički odjel, Prirodoslovno-matematički fakultet, Sveučilište u Zagrebu, 41000 Zagreb, Hrvatska

UDK 621.3.018

Originalni znanstveni rad

Po prvi put istraživana je mogućnost kaotičkog režima za robotičku jednadžbu, koristeći jednadžbu za model robota s jednim stupnjem slobode uz viskozno i suho trenje i krutosti tvrde opruge. U istraživanju nije isključeno tranzijentno gibanje. Kaotički režim je otkriven u specijalnom području parametara, s povećanom krutošću, za kritičku vrijednost parametra duljine L_c koji za 50% premašuje gornju granicu u standardnom rasponu parametara. U kaotičkom režimu otkriven je naglašeni prozor regularnosti s periodom tri.